THE JOURNAL OF BIOLOGICAL CHEMISTRY
Vol. 278, No. 2, Issue of January 10, pp. 1186–1194, 2003
© 2003 by The American Society for Biochemistry and Molecular Biology, Inc.
Printed in U.S.A.

Phosphorylation of Spinophilin Modulates Its Interaction with Actin Filaments*

Received for publication, June 10, 2002, and in revised form, October 31, 2002
Published, JBC Papers in Press, November 1, 2002, DOI 10.1074/jbc.M205754200

Linda C. Hsieh-Wilson‡§, Fabio Benfenati¶, Gretchen L. Snyder‡, Patrick B. Allen‡, Angus C. Nairn‡‖, and Paul Greengard‡**

From the ‡Laboratory of Molecular and Cellular Neuroscience, The Rockefeller University, New York, New York 10021, the §Division of Chemistry and Chemical Engineering, California Institute of Technology, Pasadena, California 91125, the ¶Department of Experimental Medicine, Section of Human Physiology, University of Genova, Genova I-16132, Italy, and the ‖Department of Psychiatry, School of Medicine, Yale University, New Haven, Connecticut 06508

Spinophilin is a protein phosphatase 1 (PP1)- and actin-binding protein that modulates excitatory synaptic transmission and dendritic spine morphology. We report that spinophilin is phosphorylated *in vitro* by protein kinase A (PKA). Phosphorylation of spinophilin was stimulated by treatment of neostriatal neurons with a dopamine D1 receptor agonist or with forskolin, consistent with spinophilin being a substrate for PKA in intact cells. Using tryptic phosphopeptide mapping, site-directed mutagenesis, and microsequencing analysis, we identified two major sites of phosphorylation, Ser-94 and Ser-177, that are located within the actin-binding domain of spinophilin. Phosphorylation of spinophilin by PKA modulated the association between spinophilin and the actin cytoskeleton. Following subcellular fractionation, unphosphorylated spinophilin was enriched in the postsynaptic density, whereas a pool of phosphorylated spinophilin was found in the cytosol. F-actin co-sedimentation and overlay analysis revealed that phosphorylation of spinophilin reduced the stoichiometry of the spinophilin-actin interaction. In contrast, the ability of spinophilin to bind to PP1 remained unchanged. Taken together, our studies suggest that phosphorylation of spinophilin by PKA modulates the anchoring of the spinophilin-PP1 complex within dendritic spines, thereby likely contributing to the efficacy and plasticity of synaptic transmission.

Dendritic spines are specialized protrusions that receive the majority of excitatory input in the central nervous system (1–3). Spines are highly motile and have been observed to change shape rapidly in response to changes in behavior, hormonal status, and synaptic activity (4–12). This dynamic behavior is believed to be fundamental to the function of dendritic spines and to contribute to the efficacy and plasticity of synaptic transmission. The ability of dendritic spines to change shape has been attributed to a dense network of proteins that facilitates the rapid assembly and disassembly of the actin cytoskeleton (13, 14). Indeed, dendritic spines contain a rich variety of receptors, ion channels, actin-regulating proteins, and other biochemical machinery that support the organization of the actin cytoskeleton (15, 16). Despite growing evidence that this protein network may be involved in the dynamic behavior of spines, the molecular mechanisms that underlie this process are not well understood.

Spinophilin (also known as neurabin II) is a PP1[1]- and actin-binding protein that is enriched in dendritic spines (17, 18). Several independent lines of evidence suggest that spinophilin may link synaptic transmission to changes in the structure and function of dendritic spines. Spinophilin has been shown to regulate excitatory synaptic transmission by targeting PP1 to α-amino-3-hydroxy-5-methyl-4-isoxazoleproprionic acid (AMPA)- and *N*-methyl-D-aspartate (NMDA)-type glutamate channels and promoting channel down-regulation through dephosphorylation (19, 20). Moreover, spinophilin-deficient mice exhibited more persistent AMPA- and NMDA-receptor currents and greatly reduced long term depression (19).

Spinophilin is likely to influence the dynamic behavior of dendritic spines by its ability to modulate the actin cytoskeleton. Spinophilin has been shown to bind and cross-link actin filaments *in vitro* (18). *In vivo*, spinophilin-deficient mice exhibited a marked increase in spine density during development (19). Moreover, cultured neurons from spinophilin knockout mice had more filopodia, or spine-like protrusions, but the same number of nerve terminals as wild-type mice. These observations suggest that spinophilin may either facilitate spine retraction or suppress the initial outgrowth of spines from the dendrite.

In addition to actin, spinophilin interacts with a variety of other proteins, including its homologue neurabin (21, 22), D2-class dopamine receptors (23), α_2-adrenergic receptors (24), and p70 S6 kinase (25). Thus, spinophilin may function as a scaffold protein to regulate cross-talk between various physiological stimuli in dendritic spines. However, it remains to be determined whether spinophilin is regulated by specific neurotransmitter systems in the brain. Notably, spinophilin contains consensus sequences for phosphorylation by several protein kinases, including protein kinase A (PKA), Ca^{2+}/calmodulin-dependent protein kinase II (CaMKII), and protein kinase C. In the present study, we demonstrate that spinophilin is phosphorylated *in vitro*, and likely, *in vivo*, by PKA, and we have

* This work was supported by United States Public Health Services Grants MH40899 and DA10044 and by Fellowship DRG-1451 of the Cancer Research Fund of the Damon Runyon-Walter Winchell Foundation (to L. C. H.-W.). The costs of publication of this article were defrayed in part by the payment of page charges. This article must therefore be hereby marked "*advertisement*" in accordance with 18 U.S.C. Section 1734 solely to indicate this fact.

** To whom correspondence should be addressed: Laboratory of Molecular and Cellular Neuroscience, The Rockefeller University, 1230 York Ave., New York, NY 10021. Tel.: 212-327-8871; Fax: 212-327-7888; E-mail: nairn@mail.rockefeller.edu.

[1] The abbreviations used are: PP1, protein phosphatase-1; PKA, protein kinase A; PSD, postsynaptic density; AMPA, α-amino-3-hydroxy-5-methyl-4-isoxazoleproprionic acid; NMDA, *N*-methyl-D-aspartate; CaMKII, Ca^{2+}/calmodulin-dependent protein kinase II; HPLC, high-performance liquid chromatography; PP2A, protein phosphatase-2A; PVDF, polyvinylidene difluoride; Ni-NTA, nickel-nitrilotriacetic acid.

This paper is available on line at http://www.jbc.org

studied the functional consequences of spinophilin phosphorylation on its interactions with actin and PP1.

EXPERIMENTAL PROCEDURES

Materials—Male Sprague-Dawley rats (150–200 g) were obtained from Charles River Laboratories (Wilmington, MA). Drugs were obtained from the following sources: cyclosporin A, okadaic acid, and calyculin A from Alexis Biochemicals (San Diego, CA); forskolin, SKF-81297 and quinpirole from Sigma-Aldrich (St. Louis, MO). The purified catalytic subunit of PP1 was kindly provided by Dr. Hsien-bin Huang (National Chung Cheng University, Taiwan). Radioisotopes were purchased from PerkinElmer Life Sciences (Boston, MA), and cellulose thin-layer chromatography plates were from Kodak (Rochester, NY). Restriction enzymes were purchased from Invitrogen (Rockville, MD) and polyvinylidene difluoride (PVDF) membrane was from Millipore (Bedford, MA). Oligonucleotides were obtained from Operon Technologies (Berkeley, CA), and peptides and phosphopeptides were synthesized at The Rockefeller University Protein/DNA Technology Center (New York, NY).

Preparation and ^{32}P Labeling of Neostriatal Slices—Neostriatal slices were prepared from male Sprague-Dawley rats (8–12 weeks old) as described previously (26). Coronal sections (500 μm in thickness) were cut on a Vibratome (Ted Pella, Redding, CA), maintained at 4 °C, and placed in cold, oxygenated (95% O_2/5% CO_2) Krebs-HCO_3^- buffer (125 mM NaCl, 5 mM KCl, 26 mM $NaHCO_3$, 1.5 mM $CaCl_2$, 1.5 mM $MgSO_4$, and 10 mM glucose, pH 7.4). Neostriatal slices were dissected from the coronal sections under a dissecting microscope and transferred individually to 2 ml of cold, oxygenated buffer. After replacing the buffer with fresh Krebs-HCO_3^- buffer, slices were preincubated at 30 °C under constant oxygenation. After 30 min, the buffer was replaced with fresh Krebs-HCO_3^- buffer containing 2.0 mCi of [^{32}P]orthophosphoric acid, and the tissue was incubated for 60 min. The radioactive buffer was then removed, and the slices were rinsed twice with 2 ml of fresh buffer. The tissue was incubated in the absence or presence of forskolin (50 μM in Krebs-HCO_3^- buffer) for 5 min. After treatment, the slices were immediately frozen in liquid nitrogen and stored at −80 °C until assayed.

Immunoprecipitation of ^{32}P-Labeled Spinophilin—Frozen tissue slices were sonicated in lysis buffer (10 mM Na_2HPO_4, pH 7.0, 150 mM NaCl, 5 mM EDTA, 1% Triton X-100, and 0.2% SDS) containing protease inhibitors (1 mM phenylmethylsulfonyl fluoride, 20 μg/ml leupeptin, 20 μg/ml antipain, 5 μg/ml pepstatin, 5 μg/ml chymostatin, 1 mM benzamidine) and phosphatase inhibitors (20 mM NaF, 1 mM Na_3VO_4, 0.05 mM Na_2MoO_4). The total [^{32}P]phosphate incorporated into trichloroacetic acid-precipitated protein was determined for each sample, and homogenates containing equal amounts of ^{32}P-labeled proteins were mixed with pre-swollen protein A-Sepharose CL-4B (10 μl per sample, Amersham Biosciences, Piscataway, NJ) for 1 h at 4 °C. The beads were then pelleted by centrifugation, and the supernatant was transferred to tubes containing a rabbit polyclonal antibody against spinophilin (3 μg of RU145 per sample (17)). The sample was mixed at 4 °C overnight and then for an additional 2 h with pre-swollen protein A-Sepharose. The beads were pelleted by centrifugation and washed four times with lysis buffer and once with 50 mM HEPES, pH 7.0. After the final wash, the beads were resuspended in SDS-PAGE sample buffer (50 mM Tris-HCl, pH 6.7, 10% glycerol, 2% SDS, 10% 2-mercaptoethanol, and 0.01% bromphenol blue), boiled for 5 min, and centrifuged. The recovered proteins were resolved by SDS-PAGE on 8% acrylamide gels. The gels were dried, and [^{32}P]phosphate incorporation into spinophilin was visualized using a PhosphorImager 400B and ImageQuaNT software from Amersham Biosciences.

Cloning and Expression of Spinophilin Fusion Proteins—A spinophilin construct containing an amino-terminal histidine tag was prepared as follows: the spinophilin sequence encoding residues 1–305 was amplified by PCR using the primers 5′-CCC ACA TAT GAT GAA GAC GGA GCC TCG-3′ and 5′-CTT TCC TCA ACC TCC ACC GGT T-3′. The resulting 900-bp fragment was digested with *Nde*I/*Xho*I and subcloned with a *Xho*I/*Xho*I fragment of spinophilin (residues 220–817 (17)) into the *Nde*I/*Xho*I site of the vector pET-15b (Novagen, Madison, WI). Point mutations were introduced using the QuikChange site-directed mutagenesis kit (Stratagene, La Jolla, CA) and the spinophilin histidine tag construct as a template. The actin-binding construct of spinophilin encoding residues 1–221 was amplified by PCR using the primers 5′-CCC ACA TAT GAT GAA GAC GGA GCC TCG-3′ and 5′-CGC GGA TCC TAC CTC GAG TCG GCT TTC TCG A-3′. The resulting fragment was digested with *Nde*I/*Bam*HI and ligated in-frame into the *Nde*I/*Bam*HI site of the vector pET-15b. All mutants were confirmed by sequencing. Recombinant proteins were expressed in bacteria and purified using nickel-nitrilotriacetic acid agarose resin (Ni-NTA; Qiagen, Valencia, CA) as described previously (27).

In Vitro Phosphorylation Reactions—Phosphorylation reactions were performed using the protein of interest (10 μM) and the catalytic subunit of PKA (40 μg/ml (28)) in 50 mM HEPES, pH 7.4, 10 mM $MgCl_2$, 1 mM EGTA at 30 °C. Reactions were initiated by the addition of ATP (50 μM) in the presence of [γ-^{32}P]ATP. The reaction was terminated at various time points by dilution of the reaction mixture into SDS-PAGE sample buffer, and the stoichiometry of phosphorylation (moles of P_i/mole of protein) was assessed after SDS-PAGE and autoradiography, by measurement of ^{32}P incorporation and normalization to the amount of protein used.

Phosphopeptide Mapping—After autoradiography, gel pieces containing ^{32}P-labeled spinophilin were re-swollen in destain (50% methanol/10% acetic acid in water), washed twice with 50% methanol in water, and dried. Gel pieces were then incubated with L-1-tosylamido-2-phenylethyl chloromethyl ketone-treated trypsin (50 μg/ml, Worthington, Lakewood, NJ) in 50 mM NH_4HCO_3, pH 8.0 (1 ml), for 18 h at 37 °C. The supernatants containing the soluble phosphopeptides were recovered after centrifugation. The extraction efficiency (~85%) was quantified by Cerenkov counting of the gel pieces and supernatants before and after digestion. Two-dimensional phosphopeptide mapping was performed as described previously (29). For phosphopeptide mapping, electrophoretic separation was at pH 3.5 for 90 min at 400 V, and ascending chromatography was in pyridine/*n*-butanol/acetic acid/water (15:10:3:12). The pattern of tryptic phosphopeptides was detected by autoradiography using PerkinElmer Life Sciences (Boston, MA) or Kodak (Rochester, NY) film.

Identification of the Phosphorylation Sites on Spinophilin—Wild-type and alanine mutant histidine fusion proteins were expressed in BL21(DE3) *Escherichia coli* by the induction of log-phase cells (5-ml cultures) with isopropyl-1-thio-β-D-galactopyranoside at 37 °C. After 1 h, cells were resuspended in ice-cold buffer (50 mM NaH_2PO_4, 300 mM NaCl, 10 mM imidazole, pH 8.0, containing protease inhibitors) and lysed by sonication. The lysate was centrifuged at 12,000 × *g* for 5 min at 4 °C, and the supernatant was mixed with Ni-NTA resin (20 μl per sample) for 30 min at 4 °C. The resin was washed three times with ice-cold buffer (50 mM NaH_2PO_4, 300 mM NaCl, 20 mM imidazole, pH 8.0) and once with 50 mM HEPES, pH 7.4, 10 mM $MgCl_2$. Phosphorylation reactions were carried out as described above with the proteins bound to the resin. After 1 h, reactions were terminated with SDS-PAGE sample buffer, and the phosphorylated proteins were loaded onto 8% acrylamide gels for autoradiography and phosphopeptide mapping analysis.

Phosphorylation sites, determined by point mutations, were confirmed by reverse phase capillary high performance liquid chromatography (HPLC) and microsequencing analysis. Wild-type spinophilin (10 μg) was phosphorylated by PKA in the presence of [γ-^{32}P]ATP. The reaction mixture was separated by SDS-PAGE and electrophoretically transferred to a PVDF membrane. The ^{32}P-labeled spinophilin was localized by autoradiography, and the membrane was excised and subjected to proteolytic digestion with trypsin or GluC proteases. Eluted peptides were separated by HPLC, and fractions eluting from the capillary column were spotted directly onto a strip of PVDF membrane using a 153 microblotter (PerkinElmer Life Sciences, Boston, MA (30)). Membrane pieces containing the ^{32}P-labeled phosphopeptides were excised and subjected to automated amino-terminal protein microsequencing and mass spectrometry.

Generation of Phosphorylation State-specific Antibodies—Rabbit polyclonal phosphorylation state-specific antibodies were generated and purified essentially as described (31). Antibodies were raised against the following cysteine-containing phosphopeptides conjugated to thyroglobulin: VRL(pS)LPRAC (residues 91–98), CLPRAS(pS)LNE (residues 95–103), and CQERA(pS)LQDRK (residues 173–182). Affinity purification was performed using dephospho- and phosphopeptides coupled to SulfoLink gel (Pierce, Rockford, IL).

Treatment of Neostriatal Slices and Immunoblotting—Neostriatal slices were dissected as described above and preincubated in fresh Krebs-HCO_3^- buffer at 30 °C under constant oxygenation. After 30 min, the slices were incubated in Krebs-HCO_3^- buffer in the absence or presence of the indicated drugs for 5–60 min. The slices were then frozen in liquid nitrogen and stored at −80 °C until assayed. Frozen tissue samples were sonicated in boiling 1% SDS containing protein phosphatase and protease inhibitors. The protein concentrations of the homogenates were determined using the BCA protein assay method (Pierce, Rockford, IL) with bovine serum albumin as a standard. Equal amounts of protein (100 μg) were separated by SDS-PAGE using 6%

acrylamide gels and transferred to PVDF membranes (0.2 μm). Membranes were blocked for 1 h in TBS (50 mM Tris-HCl, 150 mM NaCl, pH 7.4) containing 5% (w/v) nonfat dry milk and 0.1% Tween 20 and then incubated with rabbit polyclonal antibodies against spinophilin, phospho-Ser-94 spinophilin, phospho-Ser-100 spinophilin, or phospho-Ser-177 spinophilin. Following washes with TBS containing 1% nonfat milk, 0.1% Tween 20, and 0.5% bovine serum albumin, proteins were visualized by incubation with anti-rabbit horseradish peroxidase-conjugated secondary antibodies (1:5000 dilution, Pierce, Rockford, IL) and enhanced chemiluminescence (ECL) development (Amersham Biosciences, Piscataway, NJ). Chemiluminescence was detected by exposure of blots to photographic film, and bands were quantified by analysis of scanned images using Image 1.52 software (National Institutes of Health). Because the linear range for quantification of signal density by the ECL detection method is limited to <10-fold, we routinely exposed chemiluminescent membranes to film for various time periods to obtain signals within the linear range. Data were analyzed by the Mann-Whitney *U* test, with significance defined as $p < 0.05$.

Phosphorylation of Spinophilin in HEK 293T Cells and Cultured Neurons—Embryonic day 17 rat cerebrocortical or striatal tissue was used to prepare primary cortical and striatal cultures as described (32, 33). Full-length spinophilin was transiently expressed in 293T cells for 36 h following calcium phosphate transfection. Cells were treated with forskolin (50 μM) for 5 min and lysed in 1% SDS containing protease inhibitors and phosphatase inhibitors. Equal amounts of total protein were resolved on 6% acrylamide gels and analyzed by immunoblotting.

Actin Purification and Iodination—Actin was prepared from an acetone powder of rabbit skeletal muscle in buffer A (0.2 mM $CaCl_2$, 0.2 mM ATP, 0.5 mM NaN_3, 0.5 mM 2-mercaptoethanol, 2 mM Tris-HCl, pH 8.0) as described (34) and further purified by gel filtration on a Sephadex G-150 column (35). G-actin was polymerized in buffer A containing 2 mM $MgCl_2$/90 mM KCl. Polymerized actin was labeled with $Na^{125}I$ (5 mCi per 2 mg of actin) using IODO-BEADs (Pierce, Rockford, IL). ^{125}I-Labeled actin was purified over a desalting column (D-salt, Pierce, Rockford, IL) and eluted with 5 mM Tris-HCl, pH 8.0, 0.2 mM ATP, 0.2 mM $CaCl_2$, 0.5 mM dithiothreitol.

F-actin Overlays—Protein samples were separated by SDS-PAGE and transferred to nitrocellulose membranes (Schleicher & Schuell, Keene, NH). Membranes were dried for 30 min and blocked in 10 mM Tris-HCl, pH 7.4, 90 mM NaCl, 0.5% Tween 20 containing 5% nonfat dry milk for 2 h at room temperature. Membranes were incubated with ^{125}I-labeled actin (50 μg/ml) in blocking buffer containing phalloidin (5 μM, Cytoskeleton, Denver, CO) at room temperature without agitation. After 2 h, the blots were briefly washed five times with 10 mM Tris-HCl, pH 7.4, 90 mM NaCl, 0.5% Tween 20 and dried. Actin binding was quantified using a PhosphorImager 400B and ImageQuaNT software. An anti-His tag monoclonal antibody (Clontech, Palo Alto, CA) was used to detect the amount of spinophilin in each sample, and immunoreactive protein bands were quantified using ^{125}I-labeled protein A and PhosphorImager analysis.

PP1 Overlays—Protein samples were separated by SDS-PAGE and transferred to PVDF membranes. Membranes were blocked for 1 h in TBST (50 mM Tris-HCl, 150 mM NaCl, 0.05% Tween 20, pH 7.4) containing 5% nonfat milk, and then incubated with bacterially expressed PP1α (1.5 μg/ml) in 50 mM Tris-HCl, pH 7.0, 0.1 mM EGTA, 15 mM 2-mercaptoethanol, 0.01% brij-35, 0.3 mg/ml bovine serum albumin at 4 °C overnight. After washing twice with TBST containing 0.25% nonfat milk, membranes were probed with an anti-PP1α antibody (1.5 μg/ml in TBST containing 1% nonfat milk (36)) for 1 h. Following several washes, proteins were visualized by incubation with anti-rabbit horseradish peroxidase-conjugated secondary antibodies and ECL development.

F-actin Sedimentation—Phosphorylation reactions were performed on a large-scale using purified recombinant spinophilin (3 μM, ~500 μg) and in the absence or presence of PKA (40–100 μg/ml) in 50 mM HEPES, pH 7.4, 10 mM $MgCl_2$, 1 mM EGTA at 30 °C. Reactions were initiated by the addition of ATP (50 μM). An aliquot of the reaction mixture was incubated in parallel with [γ-^{32}P]ATP for determination of the phosphorylation stoichiometry (1.6 mol/mol phosphorylated approximately equally at Ser-94 and Ser-177). After 1 h, the reaction mixtures were exhaustively dialyzed into 20 mM Tris-HCl, 50 mM NaCl, pH 7.4. Immediately prior to the actin sedimentation experiments, proteins were centrifuged at 200,000 × *g* for 30 min. Protein concentrations were determined using the BCA protein assay method with bovine serum albumin as a standard.

The indicated amounts of spinophilin (62.5–1000 nM, 30 μl) were incubated with 1 μM polymerized actin (0.1 nmol actin/sample, 70 μl) for 30 min at room temperature. The samples were centrifuged at 200,000 × *g* for 30 min, and the pellet was resuspended in SDS-PAGE sample buffer and loaded onto acrylamide gels. The pelleted actin was stained with Coomassie Brilliant Blue R-250 and quantified by laser scanning densitometry. The spinophilin associated with the actin pellet was visualized by autoradiography after immunoblotting with an anti-spinophilin antibody and ^{125}I-labeled secondary antibodies and was quantified by radioactive counting of the excised bands. Samples were incubated in parallel with spinophilin (62.5–1000 nM) in the absence of actin to correct for a small amount of pelleted spinophilin in the background. Standard curves of actin and spinophilin were constructed for each analysis.

Subcellular Fractionation—The striatum of Sprague-Dawley rats was homogenized in ice-cold 0.32 M sucrose, and subcellular fractions were prepared as described (37). Proteins were resolved by SDS-PAGE and transferred to PVDF membrane. Immunoblots were probed with the indicated antibodies and visualized by ECL development.

RESULTS

Spinophilin Is Phosphorylated by PKA—The amino acid sequence of spinophilin contains consensus phosphorylation sites for several protein kinases, including PKA, protein kinase C, and Ca^{2+}/calmodulin-dependent protein kinases. To examine whether spinophilin is regulated by phosphorylation *in vivo*, striatal slices were labeled with [^{32}P]orthophosphate, and spinophilin was immunoprecipitated. A significant level of basal phosphorylation of spinophilin was detected (Fig. 1*A*). Moreover, phosphorylation was increased following treatment with the adenylyl cyclase activator, forskolin, suggesting that spinophilin might be phosphorylated by PKA *in vivo*. Two-dimensional phosphopeptide maps of spinophilin immunoprecipitated from ^{32}P-labeled slices revealed multiple phosphopeptides under basal conditions (Fig. 1*C*), as well as the appearance of novel phosphopeptides upon treatment with forskolin (peptides labeled *1*, *2*, and *4*, Fig. 1*C*).

To confirm that PKA directly phosphorylates spinophilin, we performed phosphorylation reactions *in vitro* using recombinant spinophilin, PKA, and [γ-^{32}P]ATP. Phosphorylation proceeded in a time-dependent manner and reached a maximal stoichiometry of 2.3 mol/mol within 60 min (Fig. 1*B*). The initial rate of phosphorylation was comparable to that of inhibitor-1, a physiological substrate of PKA known to be phosphorylated at a single site. Two-dimensional phosphopeptide maps of spinophilin phosphorylated by PKA to low (1-min incubation) or higher (60-min incubation) stoichiometry revealed the presence of five major phosphopeptides (labeled *1–5*, Fig. 1*D*). The phosphopeptides phosphorylated *in vitro* by PKA corresponded to the pattern of phosphopeptides phosphorylated in spinophilin in slices in response to forskolin (Fig. 1*C*) (with the exception that peptide 5 could not be detected in spinophilin phosphorylated in slices). Together, these results support the conclusion that PKA phosphorylates spinophilin *in vivo* at a subset of the total sites phosphorylated in intact cells.

Identification of the PKA Phosphorylation Sites on Spinophilin—Spinophilin contains multiple consensus sites for PKA phosphorylation within its 817-amino acid sequence. No significant phosphorylation was detected using a truncated spinophilin fragment consisting of amino acids 298–817 fused to glutathione *S*-transferase. We therefore focused on a region at the amino terminus of spinophilin (amino acids 1–221) that exhibits a high degree of homology with the actin-binding domain in neurabin (18, 21). This region was phosphorylated as efficiently as the full-length protein. Tryptic phosphopeptide maps of the amino-terminal fragment exhibited the same five major phosphopeptides as were detected using wild-type spinophilin (Fig. 1*E*), indicating that all of the PKA phosphorylation sites are located within the actin-binding domain of spinophilin.

As shown in Fig. 2*A*, the actin-binding domain contains nine consensus sites for PKA phosphorylation. To identify specific sites of phosphorylation, we compared the phosphopeptide map

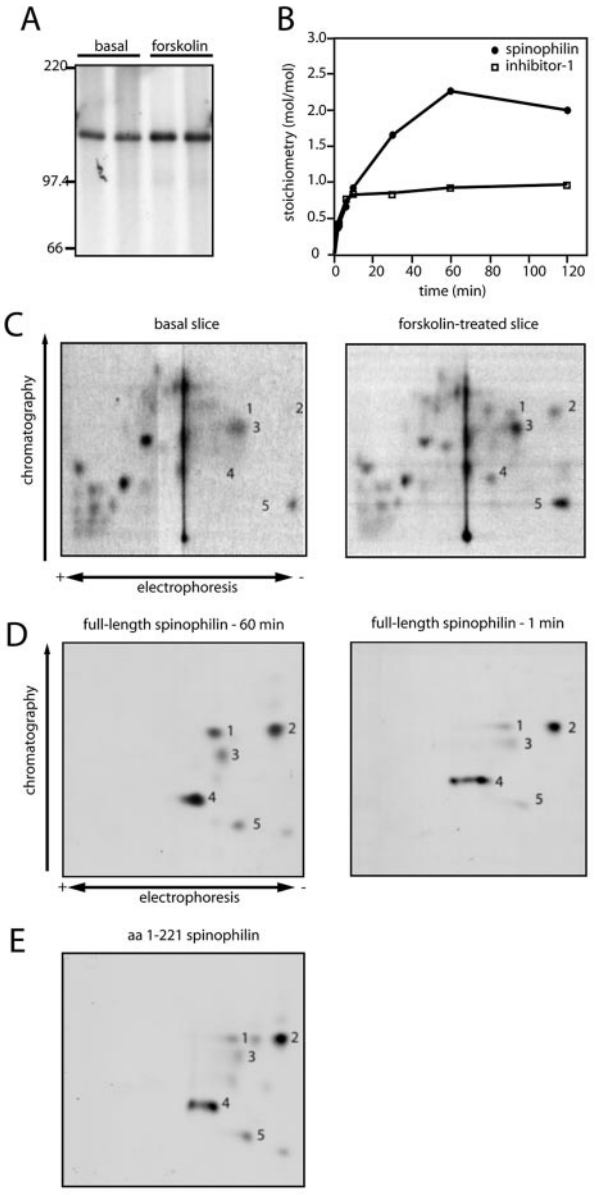

FIG. 1. **Phosphorylation of spinophilin by PKA.** *A*, spinophilin was immunoprecipitated from ^{32}P-labeled neostriatal slices treated without or with forskolin. The incorporation of [^{32}P]phosphate into spinophilin was visualized by autoradiography. *B*, time course for the *in vitro* phosphorylation of spinophilin by PKA, with comparison to inhibitor-1. Proteins were phosphorylated *in vitro* using PKA and [γ-^{32}P]ATP. The stoichiometry of phosphorylation was assessed after SDS-PAGE and autoradiography. *C*, phosphopeptide maps of spinophilin immunoprecipitated from neostriatal slices incubated without (basal slice) or with forskolin (forskolin-treated slice). Proteins were excised from gels as shown in *panel A* and digested with trypsin. The resultant phosphopeptides were separated by two-dimensional phosphopeptide mapping and visualized by autoradiography. *D*, phosphopeptide maps of spinophilin phosphorylated for 60 min (*left panel*) or 1 min (*right panel*). The autoradiograms were exposed for different times to give approximately equivalent intensities of the phosphopeptides. *E*, phosphopeptide map of the actin-binding domain of spinophilin (residues 1–221). For *D* and *E*, proteins were phosphorylated *in vitro* with PKA and [γ-^{32}P]ATP and analyzed by SDS-PAGE and two-dimensional phosphopeptide mapping. Peptides were labeled 1–5 based on the pattern observed for full-length spinophilin phosphorylated by PKA *in vitro*, with the number just to the right of the relevant phosphopeptide. In the peptide maps obtained from spinophilin phosphorylated in intact cells, peptide 5 was not consistently detected.

of wild-type spinophilin to maps of alanine mutants at each putative serine phosphorylation site. Mutant proteins were expressed as histidine fusion proteins in small-scale bacterial cultures, purified using Ni-NTA agarose, and phosphorylated with PKA and [γ-^{32}P]ATP. Mutation of Ser-94 led to the specific disappearance of phosphopeptides 1 and 2 (Fig. 2*B*, *left panel*); mutation of Ser-100 removed phosphopeptide 3 from the maps (Fig. 2*B*, *middle panel*), and mutation of Ser-177 eliminated phosphopeptides 4 and 5 (Fig. 2*B*, *right panel*). The disappearance of two phosphopeptides upon mutation of a single serine/threonine site has previously been observed (38) and most likely results from multiple tryptic cleavage sites. Interestingly, the phosphopeptide map of the Ser-94 mutant showed increased phosphorylation at Ser-100, suggesting that elimination of this primary site of phosphorylation enhances the phosphorylation kinetics of secondary sites. Mutation of all other putative phosphorylation sites (Ser-17, Ser-59, Ser-87, Ser-99, Ser-122, and Ser-126) had no effect on the phosphopeptide map patterns (data not shown).

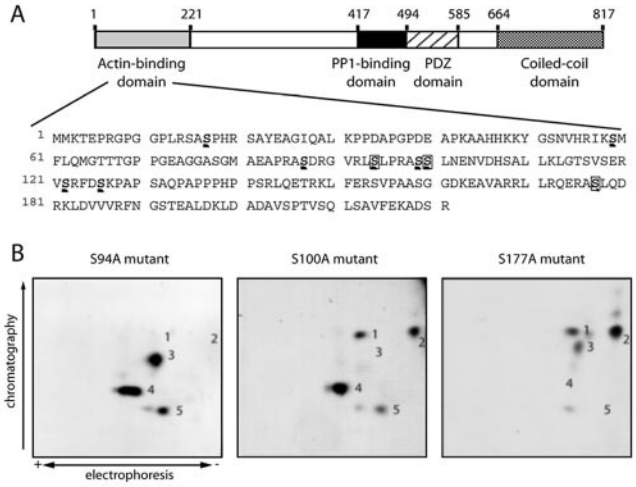

FIG. 2. **Identification of the PKA phosphorylation sites on spinophilin.** *A*, the actin-binding domain of spinophilin contains nine consensus sites for PKA phosphorylation (*underlined*). The identified sites of phosphorylation (Ser-94, Ser-100, and Ser-177) are *boxed*. *B*, two-dimensional phosphopeptide maps of alanine mutants of spinophilin (S94A, S100A, S177A).

TABLE I
Sequencing of phosphopeptides from spinophilin phosphorylated by PKA

Phosphopeptides were obtained by proteolytic cleavage of phosphorylated spinophilin. Following HPLC purification, radiolabeled peptides were identified by microsequencing and mass spectrometry. Residues in parentheses were not identified with certainty. *X* corresponds to phosphoserines (bold and underlined) or other residues that could not be sequenced.

	Peptide sequence	Amino acids
Tryptic cleavage	(L)***X***LPR	93–97
	XXXLNENVD*X*(S)(A)*X*(L)	98–111
	*X*MFLQM(G)TTTPP(G)EA. . .	59–85
Glu-C cleavage	*XA****X***LQDRKLD*X*V(V). . .	175–194

We confirmed the identity of the putative phosphorylation sites by HPLC and microsequencing analysis. Recombinant spinophilin was phosphorylated *in vitro* using PKA and [γ-^{32}P]ATP, and the tryptic phosphopeptides were purified by HPLC. Microsequencing analysis of the radiolabeled peptides identified two major peptides encompassing the Ser-94 and Ser-100 sites (amino acids 93–97 and 98–111; Table I). A third, weakly radiolabeled HPLC fraction was found to contain the peptide 59–85. Peptide 59–85 has likely co-purified with a phosphopeptide of low abundance (too low to sequence); however, we cannot rule out the possibility that this peptide contains a minor phosphorylation site that was not detected by phosphopeptide mapping. Although initial studies using the

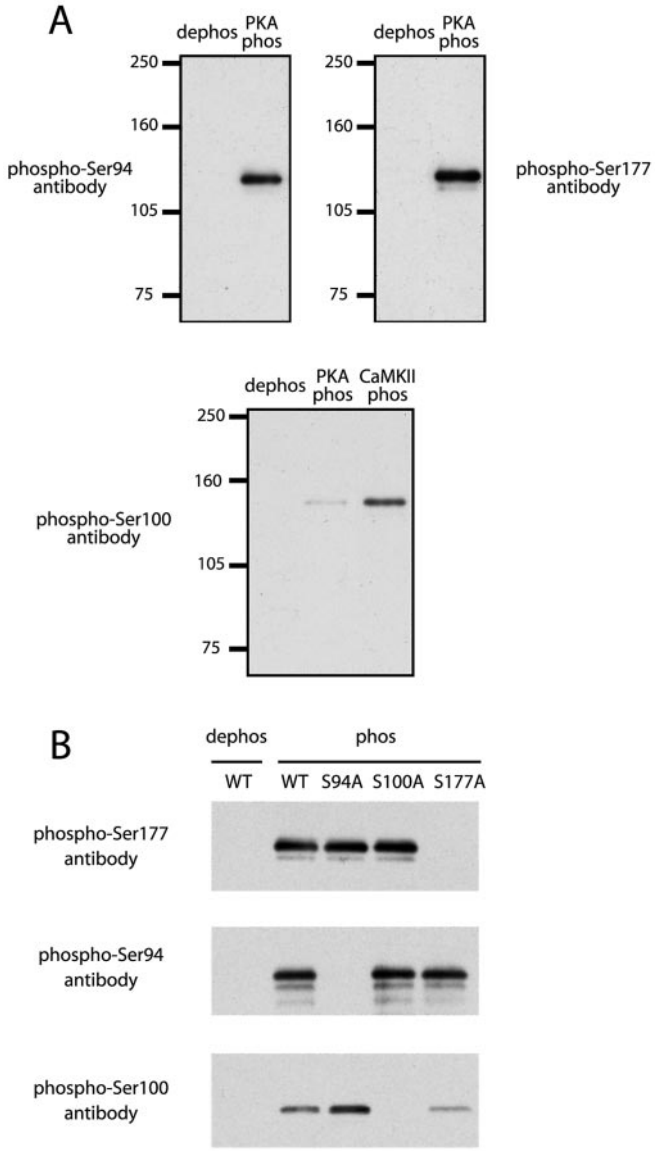

FIG. 3. **Specificity of the phosphorylation state specific antibodies.** *A*, spinophilin was phosphorylated *in vitro* without (*dephos*) or with PKA (*PKA phos*) or with CaMKII (*CaMKII phos*) as indicated, and phosphorylation state-specific antibodies to phospho-Ser-94, phospho-Ser-100, or phospho-Ser-177 were used to detect phosphorylated spinophilin by immunoblotting. *B*, the antibodies displayed no cross-reactivity toward other phosphorylated sites of spinophilin. Wild-type (*WT*) spinophilin and mutants in which Ser-94 (S94A), Ser-100 (S100A), or Ser-177 (S177A) were replaced with alanine were phosphorylated *in vitro* without (*dephos*) or with PKA or CaMKII (*phos*) as indicated. Proteins were resolved by SDS-PAGE and transferred to PVDF membranes. Samples were analyzed by immunoblotting with the phospho-Ser-94, phospho-Ser-100, or phospho-Ser-177 antibodies as indicated.

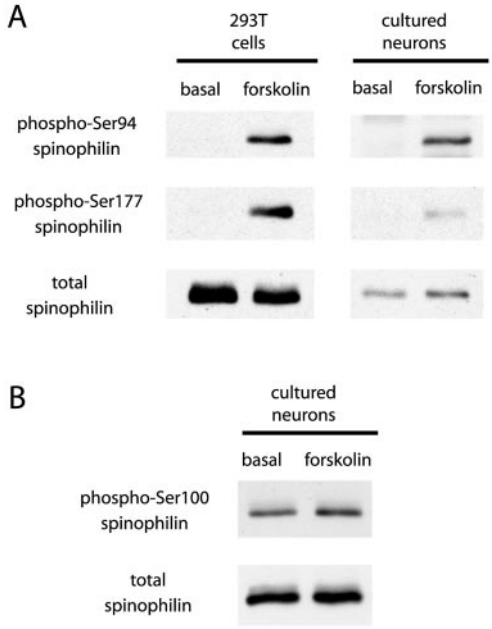

FIG. 4. **Spinophilin is phosphorylated in response to activation of PKA at Ser-94 and Ser-177 in HEK 293T cells and cultured neurons.** *A* and *B*, 293T cells, transiently transfected with spinophilin, or cultured neurons were incubated in the absence (basal) or presence of forskolin (50 μM) for 5 min. Proteins were resolved by SDS-PAGE and transferred to PVDF membranes. Spinophilin was detected by immunoblotting with the indicated antibodies.

protease trypsin did not identify a peptide encompassing Ser-177, digestion with the protease Glu-C produced a phosphopeptide that could be resolved by HPLC and identified as amino acids 175–194. Together with the phosphopeptide mapping studies, these results indicate that Ser-94 and Ser-177 of spinophilin are phosphorylated efficiently by PKA at comparable rates. In contrast, Ser-100 of spinophilin is phosphorylated by PKA at a significantly lower rate.

Phosphorylation of Ser-94 and Ser-177 of Spinophilin in Intact Cells—Having established the primary sites of phosphorylation *in vitro*, we generated phosphorylation state-specific antibodies to the Ser-94, Ser-100, and Ser-177 sites to analyze the phosphorylation of spinophilin in greater detail. The anti-phospho-Ser-94, anti-phospho-Ser-100 and anti-phospho-Ser-177 antibodies recognized spinophilin only upon phosphorylation by PKA; no detectable binding to dephosphorylated spinophilin was observed (Fig. 3*A*). Importantly, each antibody did not cross-react with the other phosphorylated site of spinophilin (Fig. 3*B*). The anti-phospho-Ser-177 antibody failed to detect phosphorylated spinophilin upon mutation of Ser-177 (but not of Ser-94) to alanine. Similarly, mutation of Ser-94 to alanine prevented anti-phospho-Ser-94, from detecting phosphorylated spinophilin. Because Ser-100 is also a putative substrate site for CaMKII, we examined the possible phosphorylation of spinophilin by CaMKII. Indeed, CaMKII phosphorylated Ser-100 of spinophilin. However, the physiological significance of this *in vitro* phosphorylation is presently unknown.

We then used the phospho-specific antibodies to examine the phosphorylation of spinophilin in both transfected HEK 293T cells and in cultured neurons. In either cell type, very low basal phosphorylation of Ser-94 and Ser-177 was observed, whereas activation of PKA with forskolin (50 μM) significantly increased the phosphorylation at both sites (Fig. 4*A*). In contrast, 1,9-dideoxy forskolin, an inactive form of forskolin, had no effect on spinophilin phosphorylation under similar conditions (data not shown). Unlike Ser-94 and Ser-177, basal phosphorylation of Ser-100 appeared to be higher in cultured neurons, and incubation with forskolin had little effect (Fig. 4*B*).

Involvement of a D1 Receptor/cAMP Cascade in Regulation of Phosphorylation of Spinophilin in Neurons—To understand further the regulation and functional significance of spinophilin phosphorylation in the brain, we identified signaling pathways that modulate spinophilin phosphorylation in the neostriatum. Rat neostriatal slices were incubated with various pharmacological agents, and the phosphorylation of spinophilin was monitored by immunoblotting of cell lysates. Because dopamine is known to stimulate adenylyl cyclase activity in the neostriatum, we evaluated the potential contribution of the two major classes of dopamine receptors, D1 and D2, on spinophilin phosphorylation. The D1 class receptors stimulate adenylyl

cyclase and increase cAMP formation (41), whereas D2 class receptors are coupled to multiple effector systems, including adenylyl cyclase, Ca^{2+} and K^+ channels, and phospholipase C (42). Treatment of neostriatal slices with the D1 receptor agonist SKF81297 increased the phosphorylation of both Ser-94 (133 ± 17% of control) and Ser-177 (236 ± 2% of control), whereas the D2 receptor agonist quinpirole had no effect on basal phosphorylation levels (Fig. 5*A*). As expected, forskolin stimulation significantly increased the phosphorylation of both Ser-94 (440 ± 20% compared with control) and Ser-177 (1030 ± 46% of control; Fig. 5*A*). These results strongly suggest that dopamine stimulates the phosphorylation of spinophilin via activation of a D1 receptor/PKA pathway.

We next examined the role of serine/threonine protein phosphatases in regulating spinophilin dephosphorylation. Neostriatal slices were incubated with cyclosporin A, a selective protein phosphatase-2B inhibitor, or with calyculin A or okadaic acid, both inhibitors of PP1 and protein phosphatase-2A (PP2A). Calyculin A, which has previously been shown to inhibit both PP1 and PP2A activity in neostriatal slices by ~40% (1 μM (43)), increased the phosphorylation of Ser-94 and Ser-177 by 5.8- and 4.4-fold, respectively (584 ± 78% and 439 ± 75% of control; Fig. 5*B*). Smaller, but significant, increases of 3.3- and 1.9-fold (332 ± 13% and 185 ± 6% of control), respectively, were produced with okadaic acid at concentrations that inhibit PP2A activity by ~80% and PP1 activity by 5% (200 nM (43)). In contrast, treatment with cyclosporin A resulted in no detectable changes in basal phosphorylation levels (102 ± 16% for Ser-94 and 95 ± 28% for Ser-177 of control). These

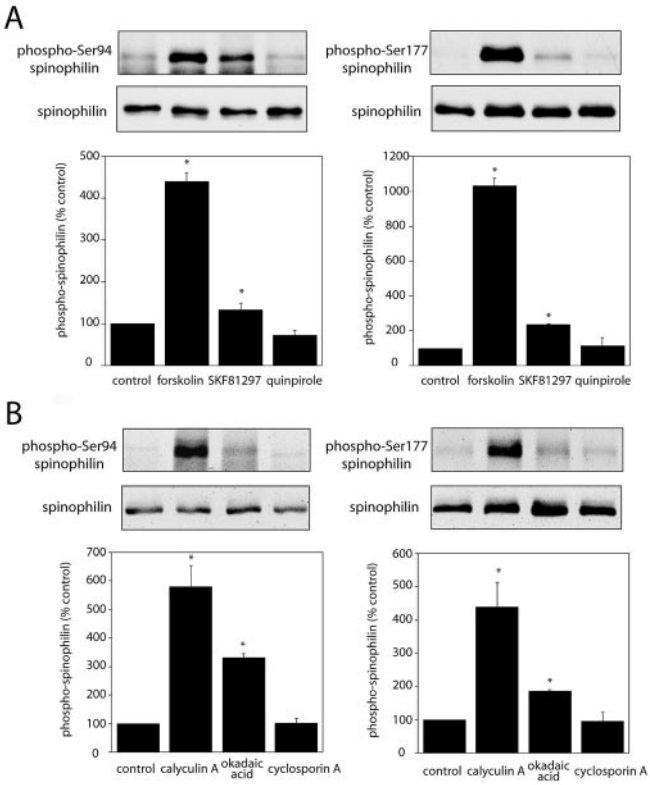

FIG. 5. **Regulation of spinophilin phosphorylation in the neostriatum.** *A*, effect of forskolin, the D1 receptor agonist SKF81297 and the D2 receptor agonist quinpirole on the phosphorylation of spinophilin. Neostriatal slices were incubated with forskolin (50 μM), SKF81297 (1 μM), or quinpirole (1 μM) for 5 min. *B*, effect of phosphatase inhibitors on the phosphorylation of spinophilin. Neostriatal slices were incubated with calyculin A (200 nM), okadaic acid (1 μM), or cyclosporin A (5 μM) for 60 min. For both *A* and *B*, the homogenates were subjected to SDS-PAGE and immunoblotted with the indicated phospho-specific antibodies. The amount of phosphorylated spinophilin was quantified by densitometry, and the data were normalized to the values obtained with untreated slices. Data represent means ± S.E. for three or four experiments. *, $p < 0.05$; Mann-Whitney *U* test compared with control.

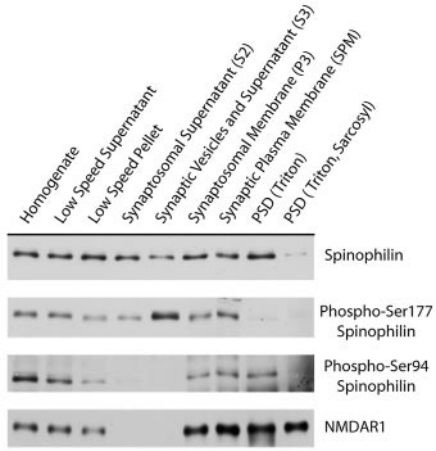

FIG. 6. **Phosphorylated spinophilin is localized to discrete subcellular compartments.** Rat neostriatal homogenates were fractionated as described under "Experimental Procedures," and the subcellular fractions were analyzed by immunoblotting with the indicated antibodies. 25 μg of total protein was loaded in each lane, with the exception of the PSD fractions, which contained 15 μg. As expected, NMDA receptor immunoreactivity was enriched in the PSD fractions.

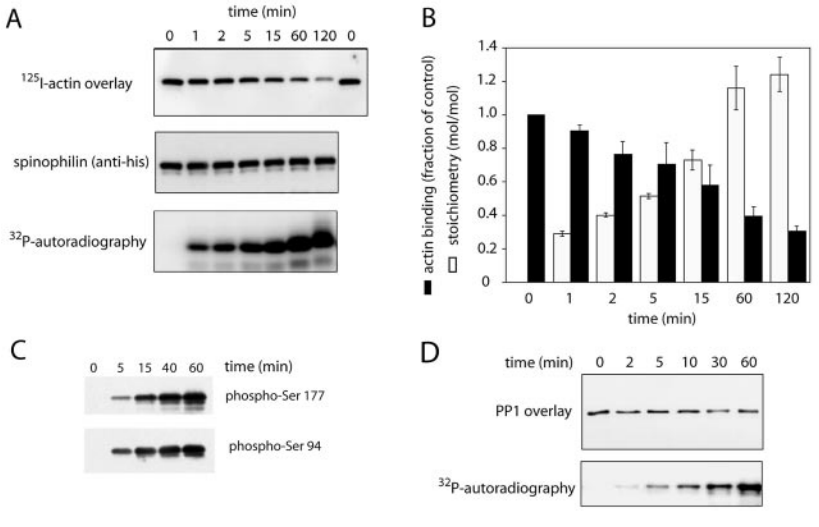

FIG. 7. **Phosphorylation disrupts the interaction of spinophilin with actin filaments but not with PP1.** Spinophilin was phosphorylated *in vitro* to various stoichiometries and examined for its ability to bind (*A*) actin filaments or (*D*) PP1. An anti-histidine tag antibody was used to detect total spinophilin levels. *B*, the phosphorylation stoichiometry and extent of actin binding were quantified using a PhosphorImager 400B and ImageQuaNT software. The values for actin binding represent the fraction of the total amount of actin bound at time zero. Data represent means ± S.E. for three experiments. *C*, the relative rates of phosphorylation of Ser-177 and Ser-94 were determined by immunoblotting aliquots of samples of spinophilin phosphorylated at different times.

data suggest that PP1, and possibly also PP2A, can reverse the PKA-mediated phosphorylation of spinophilin in the neostriatum.

Phosphorylated Spinophilin Is Enriched in Specific Subcellular Compartments—We compared the subcellular distributions of phosphorylated and unphosphorylated spinophilin by immunoblotting with anti-spinophilin, anti-phospho-Ser-94, or anti-phospho-Ser-177 antibodies. As a control, the various subcellular fractions were also probed with an antibody selective for the NMDA receptor NR1 subunit, which is enriched in postsynaptic densities. Spinophilin was found in both cytosolic and membrane-associated fractions of rat neostriatum and was highly concentrated in the PSD (Fig. 6). A single extraction (Triton X-100) of the PSD pellet did not remove spinophilin, suggesting that a significant fraction of spinophilin is tightly associated with the PSD. Similar to other targeting proteins localized to dendritic spines (44), further extraction with Sarkosyl detergent disrupted the interaction of spinophilin with the PSD.

The phosphorylated forms of spinophilin showed striking localization to specific subcellular compartments. Spinophilin phosphorylated at Ser-94 was concentrated in membrane fractions, including the PSD. In contrast, spinophilin phosphorylated at Ser-177 was absent from the PSD, although it remained associated with both the P3 and synaptic plasma membrane fraction. Importantly, spinophilin phosphorylated at Ser-177 was highly enriched in the cytosolic S3 fraction. These findings suggest that phosphorylation of spinophilin at Ser-177 reduces the ability of spinophilin to interact with one or more specific proteins in the postsynaptic density. Because phosphorylated spinophilin remains associated to some extent with the synaptic membrane, our data suggest that phosphorylation does not induce large movements in the localization of spinophilin; rather it may trigger subtle alterations in the targeting of spinophilin within dendritic spines.

The differential distributions of phospho-Ser-94 and phospho-Ser-177 spinophilin suggest that phosphorylation at each site may be differentially regulated *in vivo*. The phosphorylation studies in slices support this notion, because the Ser-177 site appeared to be more responsive to activation of PKA (10-fold *versus* 4.5-fold) than the Ser-94 site, but both sites were approximately equally responsive to inhibition of PP1/PP2A with calyculin A (Fig. 5). The greater phosphorylation of Ser-177 may reflect the different pools of PP1 and PP2A that are present in these subcellular fractions, in particular the fact that PP1 is enriched in the PSD fraction (45). Thus, the delicate balance of kinase and phosphatase activities in neurons may regulate the steady-state levels of phosphorylation at each site, thereby controlling the targeting of spinophilin within dendritic spines.

Phosphorylation of Spinophilin Reduces Its Interaction with Actin Filaments—Because the two major PKA phosphorylation sites of spinophilin, Ser-94 and Ser-177, are located within the actin binding region, we examined whether phosphorylation might influence the interaction between spinophilin and the actin cytoskeleton. Spinophilin was phosphorylated *in vitro* to various stoichiometries and examined for its ability to bind actin filaments using a ^{125}I-labeled F-actin overlay assay. Under these conditions, the stoichiometries of phosphorylation of Ser-94 and Ser-177 were approximately equal at all time points as determined by either phosphopeptide mapping (see Fig. 1*D* above) or by the use of the phospho-specific antibodies to the two sites (Fig. 7*C*). F-actin binding decreased in parallel to the increase in the level of spinophilin phosphorylation, reaching a maximum reduction of ~70% observed at a sub-maximal stoichiometry of ~1.2 mol/mol (Fig. 7, *A* and *B*). These results

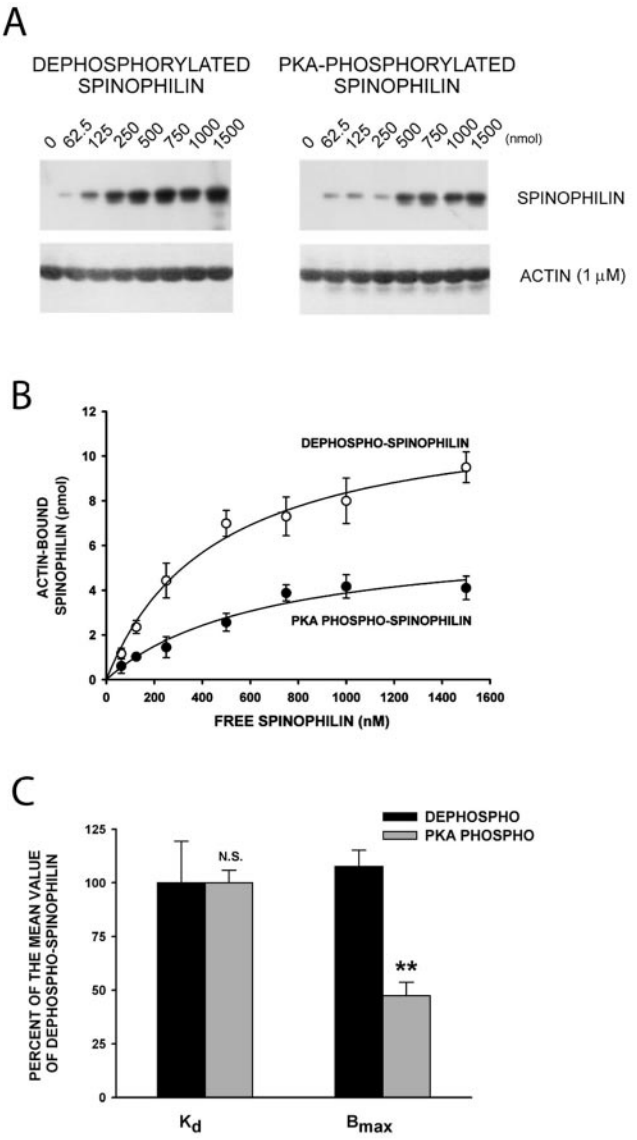

FIG. 8. **Phosphorylation decreases the stoichiometry of the spinophilin-actin interaction.** *A*, polymerized actin (1 μM) was incubated with the indicated amounts of dephosphorylated or phosphorylated spinophilin (phosphorylated to 1.6 mol/mol). Following ultracentrifugation, the amount of spinophilin associated with the actin pellet was measured by quantitative immunoblotting. *B* and *C*, binding isotherms (*B*) indicate that phosphorylation markedly decreases the binding stoichiometry (B_{max}) without affecting the dissociation constant (K_d) of the spinophilin-actin interaction (*C*). Data represent means ± S.E. for three experiments.

suggest that phosphorylation by PKA directly disrupts the association between spinophilin and F-actin.

We further analyzed the interaction of phosphorylated spinophilin with actin filaments by performing co-sedimentation studies. Spinophilin was phosphorylated by PKA to a stoichiometry of 1.6 mol/mol and incubated with polymerized actin. For comparison, unphosphorylated spinophilin was analyzed in parallel. Following ultracentrifugation, the amount of spinophilin associated with the actin pellet was measured by quantitative immunoblotting (Fig. 8). The analysis of the binding isotherms indicated that phosphorylation did not alter the binding affinity of spinophilin for F-actin: dephospho- and phospho-spinophilin exhibited similar dissociation constants of 455 ± 88 and 490 ± 35 nM, respectively. These values are close to the K_d of 500 nM previously reported for dephospho-spinophilin (18). In contrast, the stoichiometry of the spinophilin-actin

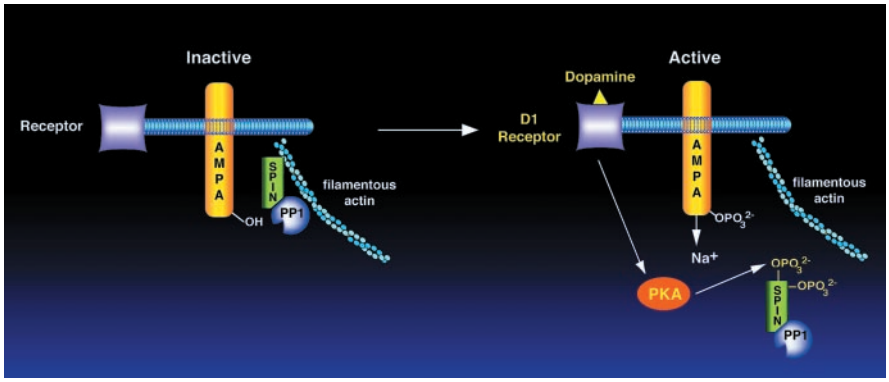

FIG. 9. **Model for the regulation of AMPA-type glutamate receptors by spinophilin.** Spinophilin anchors PP1 in the vicinity of the AMPA channel by binding to actin filaments. Under basal conditions, the spinophilin-PP1 complex maintains the AMPA channel in a dephosphorylated state in which it is relatively insensitive to its neurotransmitter, glutamate. After D1 receptor stimulation, AMPA channel phosphorylation is increased due to phosphorylation of spinophilin by PKA, likely targeted close to the synapse via protein kinase A-anchoring proteins. In turn, the spinophilin-PP1 complex is removed from the vicinity of the channel and leads to synergistic increases in phosphorylation of the AMPA receptor.

interaction decreased by 53% upon phosphorylation (B_{max} of 12 ± 0.7 mol/mol for dephospho-spinophilin, 5.7 ± 0.8 mol/mol for phospho-spinophilin, $p < 0.003$). Phosphorylation of spinophilin did not appear to perturb the G- to F-actin equilibrium (data not shown), consistent with the binding of spinophilin to the sides rather than the ends of actin filaments (18).

In addition to associating with actin, spinophilin binds to PP1 and inhibits its activity *in vitro*. We therefore investigated whether phosphorylation might modulate the interaction of spinophilin with PP1. Phosphorylation of spinophilin by PKA, however, had no detectable effect on PP1 binding in overlay assays (Fig. 7*D*). Taken together, these results strongly suggest that the phosphorylation of spinophilin by PKA regulates its association with the actin cytoskeleton, without disrupting the spinophilin-PP1 complex.

DISCUSSION

We have provided the first demonstration that protein kinases modulate the function of spinophilin in neurons. Our data indicate that spinophilin is phosphorylated by PKA *in vitro* at Ser-94 and Ser-177, which are located within the actin-binding domain of spinophilin. Ser-94 and Ser-177 are contained within consensus sites for phosphorylation by PKA and are phosphorylated in neurons in response to activation of D1 dopamine receptors or forskolin, consistent with both sites being physiological targets for PKA in intact cells. Ser-100 was identified as a minor site for PKA *in vitro* but was not regulated by activation of PKA *in vivo*. Interestingly, Ser-94 and Ser-177 of spinophilin are not conserved in neurabin, a homologue of spinophilin that shares ~48% amino acid identity with spinophilin. This observation suggests that the functional activities of spinophilin and neurabin may be differentially regulated through protein phosphorylation. Indeed, neurabin is phosphorylated *in vitro* by PKA at a specific site that is not found in spinophilin, and phosphorylation appears to decrease the association of neurabin with PP1 (46).

Phosphorylation of spinophilin by PKA disrupts its ability to associate with actin filaments. Interestingly, phosphorylated spinophilin bound to F-actin with high affinity, but with reduced stoichiometry. These findings suggest that the actin binding region of spinophilin contains at least two distinct recognition sites for actin. In support of this idea, we have observed that the actin-binding domain of spinophilin (amino acids 1–221) is sufficient to bundle actin filaments.[2] Phosphorylation of spinophilin may disrupt one of these sites, reducing the number of actin molecules bound to spinophilin without perturbing the binding affinity of spinophilin for F-actin. Several actin bundling proteins, including α-actinin, dystrophin, and spectrin, possess multiple actin-binding domains, which contact actin molecules via α-helical structures (47–49). Under the conditions used in the present study, both Ser-94 and Ser-177 were phosphorylated to approximately equal levels. Ser-94 and Ser-177 reside in regions predicted to adopt α-helices, and phosphorylation of spinophilin at either or both sites may prevent the binding of actin molecules through destabilization of the protein-protein interface.

Phosphorylation of spinophilin was associated with decreased binding to the post-synaptic density. In contrast to unphosphorylated spinophilin, spinophilin phosphorylated at Ser-177 was absent from the PSD and was enriched in the cytosolic fractions. This striking difference in subcellular localization suggests that phosphorylation triggers changes in the targeting of spinophilin within dendritic spines. Although it is possible that the pool of spinophilin associated with the PSD cannot be phosphorylated by PKA, we consider this possibility unlikely. Several protein kinase A anchoring proteins have been shown to target PKA to the PSD (50, 51) and enable the kinase to phosphorylate proteins such as the GluR1 subunit of AMPA receptors (26), NMDA channels (52, 53), and other receptors. Moreover, phosphorylation of spinophilin at the Ser-94 site was shown to occur in the PSD. Taken together with our actin-binding studies, the altered subcellular distribution of phosphorylated spinophilin supports the notion that PKA activation dynamically modulates the localization of spinophilin within dendritic spines.

Our previous studies have shown in striatal neurons that spinophilin plays a role in the regulation of AMPA channels by the dopamine D1 receptor/cAMP/DARPP-32 cascade (19, 20). This is believed to result from an amplification process that involves both direct phosphorylation of the channel by PKA and inhibition of PP1 activity via PKA-mediated phosphorylation of DARPP-32. In these studies, we also observed that AMPA currents were stabilized by perfusion into neurons of a synthetic spinophilin peptide that disrupts the targeting of PP1 to spinophilin (20). This latter result implicated spinophilin in the localized targeting of active PP1 close to AMPA channels. In the present study, we have found that phosphorylation by PKA perturbed the interaction of actin with spinophilin, but that it had no effect on the binding of PP1 to spinophilin. Thus, activation of cAMP-dependent signaling would be expected to alter the association of the spinophilin-PP1 complex with the actin cytoskeleton. Phosphorylation of spinophilin by PKA may therefore contribute to the increased phosphorylation of AMPA channels by also altering the localization of PP1 (Fig. 9).

[2] L. C. Hsieh-Wilson and P. Greengard, unpublished observations.

The ability of cAMP-dependent signaling cascades to alter dynamically the localization of the spinophilin-PP1 complex may also have important consequences for synaptic plasticity. PP1 has been found to play a role in synaptic plasticity likely by modulating AMPA type glutamate channels important for synaptic transmission, and targeting of PP1 has been proposed to play a role in long term depression (54, 55). Spinophilin knockout mice exhibit altered glutamatergic transmission and reduced long term depression (19), suggesting that spinophilin is responsible for the regulation of AMPA receptors by PP1. Phosphorylation of spinophilin by PKA may contribute to regulation of ion channel conductances critical for the maintenance and plasticity of dendritic spines (56, 57). Phosphorylation of spinophilin may also influence trafficking of AMPA receptors by modulating the actin cytoskeleton in dendritic spines.

Spinophilin phosphorylation could have other important consequences for the structure and function of dendritic spines. Changes in the number, size, and shape of dendritic spines have been associated with learning, electrophysiological, developmental, and hormonal changes (4–12). The ability of dendritic spines to change shape has been attributed to a dense network of proteins that facilitates the rapid assembly and disassembly of the actin cytoskeleton (13, 14). Spinophilin has been shown to cross-link actin filaments *in vitro* and to regulate the development of dendritic spines *in vivo* (19). Thus, phosphorylation of spinophilin may influence the morphology of spines by modulating the bundling or polymerization of actin filaments. Alternatively, phosphorylation may serve to control PP1-mediated changes in the actin cytoskeleton. Previous studies have shown that PP1 regulates cellular morphology through dephosphorylation of the actin cytoskeleton (58–60).

In conclusion, we have demonstrated that phosphorylation of spinophilin is increased in response to dopamine D1 receptor/cAMP signaling cascades. Spinophilin phosphorylation, in turn, modulates its ability to interact with the actin cytoskeleton. Our findings suggest that phosphorylation of spinophilin by PKA regulates anchoring of the spinophilin-PP1 complex within dendritic spines. These studies may provide greater insight into the molecular mechanisms that underlie synaptic plasticity and dendritic spine morphology. Future studies will examine the dynamic targeting of the spinophilin-PP1 complex in living neurons and its impact on the structure and function of dendritic spines.

Acknowledgments—We thank Martin Lan, Mercedes Paredes, Dr. Stacie Grossman, Jean Whitesell (Cocalico Biologicals, Inc.), and Dr. Joseph Fernandez (Rockefeller University Protein/DNA Technology Center) for valuable assistance.

REFERENCES

1. Harris, K. M. (1999) *Curr. Opin. Neurobiol.* **9,** 343–348
2. Kirov, S. A., and Harris, K. (1999) *Nat. Neurosci.* **2,** 878–883
3. Gray, E. G. (1959) *J. Anat.* **83,** 420–433
4. Horn, G., Bradley, P., and McCabe, B. J. (1985) *J. Neurosci.* **5,** 3161–3168
5. Moser, M. B., Trommald, M., and Andersen, P. (1994) *Proc. Natl. Acad. Sci. U. S. A.* **91,** 12673–12675
6. Woolley, C. S., Weiland, N. G., McEwen, B. S., and Schwartzkroin, P. A. (1997) *J. Neurosci.* **17,** 1848–1859
7. Boyer, C., Schikorski, T., and Stevens, C. F. (1998) *J. Neurosci.* **18,** 5294–5300
8. Dunaevsky, A., Tashiro, A., Majewska, A., Mason, C., and Yuste, R. (1999) *Proc. Natl. Acad. Sci. U. S. A.* **96,** 13438–13443
9. Harris, K. M., Jensen, F. E., and Tsao, B. (1992) *J. Neurosci.* **12,** 2685–2705
10. Maletic-Savatic, M., Malinow, R., and Svoboda, K. (1999) *Science* **283,** 1923–1927
11. Engert, F., and Bonhoeffer, T. (1999) *Nature* **399,** 66–70
12. Lendvai, B., Stern, E. A., Chen, B., and Svoboda, K. (2000) *Nature* **404,** 876–881
13. Matus, A. (2000) *Science* **290,** 754–758
14. Halpain, S. (2000) *Trends Neurosci.* **23,** 141–146
15. Kim, J. H., and Huganir, R. L. (1999) *Curr. Opin. Cell Biol.* **11,** 248–254
16. Lee, S. H., and Sheng, M. (2000) *Curr. Opin. Neurobiol.* **10,** 125–131
17. Allen, P. B., Ouimet, C. C., and Greengard, P. (1997) *Proc. Natl. Acad. Sci. U. S. A.* **94,** 9956–9961
18. Satoh, A., Nakanishi, H., Obaishi, H., Wada, M., Takahashi, K., Satoh, K., Hirao, K., Nishioka, H., Hata, Y., Mizoguchi, A., and Takai, Y. (1998) *J. Biol. Chem.* **273,** 3470–3475
19. Feng, J., Yan, Z., Ferreira, A., Tomizawa, K., Liauw, J. A., Zhuo, M., Allen, P. B., Ouimet, C. C., and Greengard, P. (2000) *Proc. Natl. Acad. Sci. U. S. A.* **97,** 9287–9292
20. Yan, Z., Hsieh-Wilson, L., Feng, J., Tomizawa, K., Allen, P. B., Fienberg, A. A., Nairn, A. C., and Greengard, P. (1999) *Nat. Neurosci.* **2,** 13–17
21. Nakanishi, H., Obaishi, H., Satoh, A., Wada, M., Mandai, K., Satoh, K., Nishioka, H., Matsuura, Y., Mizoguchi, A., and Takai, Y. (1997) *J. Cell Biol.* **139,** 951–961
22. MacMillan, L. B., Bass, M. A., Cheng, N., Howard, E. F., Tamura, M., Strack, S., Wadzinski, B. E., and Colbran, R. (1999) *J. Biol. Chem.* **274,** 35845–35854
23. Smith, F. D., Oxford, G. S., and Milgram, S. L. (1999) *J. Biol. Chem.* **274,** 19894–19900
24. Richman, J. G., Brady, A. E., Wang, Q., Hensel, J. L., Colbran, R. J., and Limbird, L. E. (2001) *J. Biol. Chem.* **276,** 15003–15008
25. Burnett, P., Blackshaw, S., Lai, M. M., Qureshi, I. A., Burnett, A. F., Sabatini, D. M., and Snyder, S. H. (1998) *Proc. Natl. Acad. Sci. U. S. A.* **98,** 8351–8356
26. Snyder, G., Allen, P., Fienberg, A., Valle, C., Huganir, R., Nairn, A., and Greengard, P. (2000) *J. Neurosci.* **20,** 4480–4488
27. Hsieh-Wilson, L. C., Allen, P. B., Watanabe, T., Nairn, A. C., and Greengard, P. (1999) *Biochemistry* **38,** 4365–4373
28. Kaczmarek, L. K., Jennings, K. R., Strumwasser, F., Nairn, A. C., Walter, U., Wilson, F. D., and Greengard, P. (1980) *Proc. Natl. Acad. Sci. U. S. A.* **77,** 7487–7491
29. Nairn, A. C., and Greengard, P. (1987) *J. Biol. Chem.* **262,** 7273–7281
30. Bibb, J. A., Nishi, A., O'Callaghan, J. P., Ule, J., Lan, M., Snyder, G. L., Horiuchi, A., Saito, T., Hisanaga, S., Czernik, A. J., Nairn, A. C., and Greengard, P. (2001) *J. Biol. Chem.* **276,** 14490–14497
31. Czernik, A. J., Mathers, J., and Mische, S. M. (1997) *Neuromethods* **30,** 219–246
32. Gouras, G. K., Xu, H., Jovanovic, J. N., Buxbaum, J. D., Wang, R., Greengard, P., Relkin, N. R., and Gandy, S. (1998) *J. Neurochem.* **71,** 1920–1925
33. Petersen, A., Larsen, K. E., Behr, G. G., Romero, N., Przedborski, S., Brundin, P., and Sulzer, D. (2001) *Hum. Mol. Genet.* **10,** 1243–1254
34. Spudich, J. A., and Watt, S. (1971) *J. Biol. Chem.* **246,** 4866–4871
35. MacLean-Fletcher, S., and Pollard, T. D. (1980) *Biochem. Biophys. Res. Commun.* **96,** 18–27
36. da Cruz e Silva, E., Fox, C. A., Ouimet, C. C., Gustafson, E., Watson, S. J., and Greengard, P. (1995) *J. Neurosci.* **15,** 3375–3389
37. Jones, D. H., and Matus, A. I. (1974) *Biochim. Biophys. Acta* **356,** 276–287
38. Paul, S., Snyder, G. L., Yokakura, H., Picciotto, M. R., Nairn, A. C., and Lombroso, P. J. (2000) *J. Neurosci.* **20,** 5630–5638
39. Molloy, S. S., and Kennedy, M. B. (1991) *Proc. Natl. Acad. Sci. U. S. A.* **88,** 4756–4760
40. Ocorr, K. A., and Schulman, H. (1991) *Neuron* **6,** 907–914
41. Stoof, J. C., and Kebabian, J. W. (1981) *Nature* **294,** 366–368
42. Huff, R. M. (1996) *Cell Signalling* **8,** 453–459
43. Nishi, A., Snyder, G. L., Nairn, A. C., and Greengard, P. (1999) *J. Neurochem.* **72,** 2015–2021
44. Penzes, P., Johnson, R. C., Sattler, R., Zhang, X., Huganir, R. L., Kambampati, V., Mains, R. E., and Eipper, B. A. (2001) *Neuron* **29,** 229–242
45. Ouimet, C. C., da Cruz e Silva, E., and Greengard, P. (1995) *Proc. Natl. Acad. Sci. U. S. A.* **92,** 3396–3400
46. McAvoy, T., Allen, P. B., Obaishi, H., Nakanishi, H., Takai, Y., Greengard, P., Nairn, A. C., and Hemmings, H. C., Jr. (1999) *Biochemistry* **38,** 12943–12949
47. Vanderkerckhove, J., and Vancompernolle, K. (1992) *Curr. Opin. Cell Biol.* **4,** 34–42
48. Volkmann, N., DeRosier, D., Matsudaira, P., and Hanein, D. (2001) *J. Cell Biol.* **153,** 947–956
49. Galkin, V. E., Orlova, A., VanLoock, M. S., Rybakova, I. N., Ervasti, J. M., and Egelman, E. H. (2002) *J. Cell Biol.* **157,** 243–251
50. Colledge, M., and Scott, J. D. (1999) *Trends Cell Biol.* **9,** 216–221
51. Carr, D. W., Stofkohahn, R. E., Fraser, I. D. C., Cone, R. D., and Scott, J. D. (1992) *J. Biol. Chem.* **267,** 16816–16823
52. Snyder, G. L., Fienberg, A. A., Huganir, R. L., and Greengard, P. (1998) *J. Neurosci.* **18,** 10297–10303
53. Leonard, A. S., and Hell, J. W. (1997) *J. Biol. Chem.* **272,** 12107–12115
54. Mulkey, R. M., Endo, S., Shenolikar, S., and Malenka, R. C. (1994) *Nature* **369,** 486–488
55. Morishita, W., Connor, J. H., Xia, H., Quinlan, E. M., Shenolikar, S., and Malenka, R. C. (2001) *Neuron* **32,** 1133–1148
56. McKinney, R. A., Capogna, M., Durr, R., Gahwiler, B. H., and Thompson, S. M. (1999) *Nat. Neurosci.* **2,** 44–49
57. Fischer, M., Kaech, S., Wagner, U., Brinkhaus, H., and Matus, A. (2000) *Nat. Neurosci.* **3,** 887–894
58. Fernandez, A., Brautigan, D. L., Mumby, M., and Lamb, N. J. (1990) *J. Cell Biol.* **111,** 103–112
59. Inada, H., Togashi, H., Nakamura, Y., Kaibuchi, K., Nagata, K., and Inagaki, M. (1999) *J. Biol. Chem.* **274,** 34932–34939
60. Hartshorne, D. J. (1998) *Acta Physiol. Scand.* **164,** 483–493